Closing in on the tip of the CMSSM stau coannihilation strip

Nishita Desai,[1] John Ellis,[2,3] Feng Luo,[2] and Jad Marrouche[4]

[1]*Institut für theoretische Physik, Universität Heidelberg, Heidelberg 69120, Germany*
[2]*Theoretical Particle Physics and Cosmology Group, Department of Physics, King's College London,
London WC2R 2LS, United Kingdom*
[3]*Theory Division, CERN, CH-1211 Geneva 23, Switzerland*
[4]*Physics Department, CERN, CH-1211 Geneva 23, Switzerland*

Near the tip of the $\tilde{\tau}$ coannihilation strip in the CMSSM with a neutralino lightest supersymmetric particle χ, the astrophysical cold dark matter density constraint forces the $\tilde{\tau} - \chi$ mass difference to be small. If this mass difference is smaller than m_τ, the $\tilde{\tau}$ may decay either in the outer part of an LHC detector—the "disappearing track" signature—or be sufficiently long-lived to leave the detector before decaying—the long-lived massive charged-particle signature. We combine searches for these signatures with conventional E_T^{miss} searches during LHC Run 1, identifying the small remaining parts of the CMSSM $\tilde{\tau}$ coannihilation strip region that have not yet been excluded and discussing how they may be explored during Run 2 of the LHC.

I. INTRODUCTION

A major theme of the searches for new physics during Run 1 of the LHC at 7 and 8 TeV in the center of mass has been the search for supersymmetry via various experimental signatures [1,2]. The constraints imposed by the absences of any statistically significant excesses of events with such signatures are frequently interpreted assuming that *R*-parity is conserved, in which case the lightest supersymmetric particle (LSP) could be present today as a cosmological relic [3] from the big bang, and many astrophysical constraints also come into play. Foremost among these is the density of cold dark matter [4,5], which imposes restrictions on supersymmetric model parameters that are often respected only in narrow strips in the supersymmetric parameter space. This is the case, for example, if it is assumed that the LSP is the lightest neutralino χ. In particular, in the minimal supersymmetric extension of the Standard Model with soft supersymmetry-breaking parameters $m_{1/2}, m_0$ and A_0 assumed to be universal at the grand unification scale (the CMSSM) [6,7], the cold dark matter density constraint is respected along strips where χ coannihilation with the lighter $\tilde{\tau}$ slepton [8] or the lighter $\tilde{t}$ squark [9] is important, or where $\chi - \chi$ annihilation is enhanced by a direct-channel Higgs resonance [6,10], or an enhanced Higgsino component in the composition of the LSP χ [11].

As discussed in previous papers [12–14], the $\tilde{\tau} - \chi$ coannihilation strip region in the CMSSM is particularly accessible to supersymmetry searches at the LHC. However, complete exploration of this region requires a combination of different search strategies. As the tip of the $\tilde{\tau} - \chi$ coannihilation strip is approached at large $m_{1/2}$, the $\tilde{\tau} - \chi$ mass difference Δm becomes very small. If

$\Delta m > m_\tau$, the $\tilde{\tau}$ and other heavier sparticles decay rapidly into the LSP χ, providing a classical E_T^{miss} signature. However, if $\Delta m < m_\tau$ the $\tilde{\tau}$ lifetime becomes so long that it may decay in the outer part of a generic LHC detector— the "disappearing track" signature—or even outside the detector altogether, in which case the $\tilde{\tau}$ would appear as a slow-moving massive, penetrating charged particle. Full exploration of the CMSSM $\tilde{\tau} - \chi$ coannihilation strip therefore requires a careful combination of searches for these signatures as well as for E_T^{miss}.

In a previous paper [12], the principal decay rates and the lifetime of the $\tilde{\tau}$ in the CMSSM when $\Delta m < m_\tau$ were reevaluated, and the impact on the CMSSM of the Run 1 LHC searches for massive metastable charged particles were analyzed. Subsequently, updated LHC results from searches for such particles have been made available [15], as well as searches for E_T^{miss} events [16] and disappearing tracks [17]. The purpose of this paper is to make a combined analysis of these different searches within the CMSSM, identify the remaining regions of the CMSSM $\tilde{\tau}$ coannihilation strip, and discuss how they may be explored in Run 2 of the LHC.

In Sec. II of this paper we first review relevant features of the $\tilde{\tau}$ coannihilation strip region within the CMSSM, which extends up to $m_{1/2} \sim 1300$ GeV for $\tan\beta = 40$ and $A_0 > 0$. We then review the calculations of $\tilde{\tau}$ decays when $\Delta m < m_\tau$, which indicate that the dominant $\tilde{\tau}$ signature would be a massive metastable charged particle if $\Delta m \lesssim 1.2$ GeV and a disappearing track if $\Delta m \gtrsim 1.2$ GeV.

In Sec. III we discuss the impacts of the relevant LHC Run 1 searches for new physics, including regions where the relic LSP density is less than the total cold dark matter density, as would be allowed if there is another component of the astrophysical cold dark matter. We first discuss the

E_T^{miss} searches, which exclude the relevant portions of the CMSSM parameter space where $\Delta m > m_\tau$ and $m_{1/2} < 780$ GeV. For $\tan\beta = 10$, these searches exclude the portion of the $\tilde{\tau}$ coannihilation strip where $\Delta m \gtrsim 3$ GeV, whereas Δm as large as 9 GeV can be allowed for $\tan\beta = 40$. We then update our previous analysis of the metastable $\tilde{\tau}$ case, finding that the most recent LHC Run 1 search for such particles excludes $m_{1/2} \lesssim 800$ GeV to $\lesssim 1100$ GeV for $\Delta m \lesssim 1.2$ GeV, depending on the value of $\tan\beta$ and A_0. We then analyze the impact of the disappearing track search on the intermediate band where $m_\tau > \Delta m \gtrsim 1.2$ GeV, using PYTHIA 8 [18,19] to simulate $\tilde{\tau}$ decays in an LHC detector outside the beam pipe. We find that this search is weaker than the other constraints, yielding $m_{1/2} \gtrsim 400$ GeV.

In Sec. IV we discuss the interplay of these different searches, as well as the constraints from the observed value of the Higgs mass m_h [20,21], calculated using the recently released FEYNHIGGS 2.10.0 [22].

In Sec. V we consider the sensitivities of LHC Run 2 searches with 300/fb of integrated luminosity at 14 TeV in the center of mass. The conventional E_T^{miss} searches should have sufficient sensitivity to find evidence for supersymmetry or to exclude the coannihilation region of the CMSSM if $\Delta m > m_\tau$. Likewise, searches for massive metastable charged particles should be able to find evidence for the $\tilde{\tau}$ or to exclude the coannihilation region of the CMSSM if $\Delta m \lesssim 1.2$ GeV. However, simple extrapolation of the current disappearing track searches indicates that they would have insufficient sensitivity to exclude or find evidence for supersymmetry if $m_\tau > \Delta m \gtrsim 1.2$ GeV, so we consider ways in which the sensitivity of future such searches could be enhanced.

Finally, Sec. VI summarizes our conclusions.

II. THE $\tilde{\tau}$ COANNIHILATION STRIP AND ITS DECAYS WITHIN THE CMSSM

A. Anatomy of the stau coannihilation strip region

The focus of our attention in this paper is the CMSSM, in which R-parity is conserved and it is assumed that universal soft supersymmetry-breaking parameters $m_{1/2}, m_0$ and A_0 are input at the GUT scale. We assume that the stable LSP is the lightest neutralino χ, giving priority to the CMSSM parameter region near the strip where its astrophysical relic density is brought into the range $0.115 < \Omega_\chi h^2 < 0.125$ [5] that is acceptable within conventional cosmology by coannihilation with the lighter tau-slepton $\tilde{\tau}$ and other, heavier sleptons, but also considering smaller values of Δm that yield lower values of $\Omega_\chi h^2$. Our objective is to study the extent to which this simplest supersymmetric scenario has been explored with data from Run 1 of the LHC at 7 and 8 TeV in the center of mass, and the extent to which it can be explored further with future LHC data at 14 TeV. As we discuss, even this simplest scenario has rich

phenomenological possibilities beyond the standard E_T^{miss} signatures, posing challenges for its complete exploration.

As is well known, as $m_{1/2}$ increases toward the tip of the stau coannihilation strip the $\tilde{\tau} - \chi$ mass difference Δm decreases monotonically towards zero, which is attained at $m_{1/2} = \mathcal{O}(1000)$ GeV, the maximum value of $m_{1/2}$ depending on the values of $\tan\beta$ and A_0. In this paper, we use consistently SOFTSUSY 3.3.7 [23] to calculate the sparticle spectrum, and the latter is passed to MICROMEGAS 3.5.5 [24] to calculate $\Omega_\chi h^2$. Fig. 1 displays bands with $\Delta m \leq 5$ GeV for values of $m_{1/2}$ close to the tips of the coannihilation strips for $\tan\beta = 10$ (upper panels) and 40 (lower panels), in each case for the two choices $A_0 = 0$ (left panels) and $2.5m_0$ (right panels). The choices of $\tan\beta$ are representative of the larger and smaller values found in the coannihilation region in a recent global analysis of the CMSSM parameter space [25], and the restriction to $A_0 \geq 0$ is motivated by the Higgs boson mass m_h measured at the LHC, which is easier to reproduce for positive values of A_0.[1] The coannihilation strips where $0.115 < \Omega_\chi h^2 < 0.125$ are shown as pink bands. We see that the strips for $\tan\beta = 10$ terminate when $\Delta m \to 0$ at $m_{1/2} \simeq 900$–950 GeV, with little sensitivity to A_0, whereas the strips for $\tan\beta = 40$ and $A_0 = 0(2.5m_0)$ extend to larger $m_{1/2} \simeq 1150$–1200 GeV (1300–1350 GeV). We also see that Δm drops below m_τ for $m_{1/2} \simeq 800$–850 GeV for $\tan\beta = 10$, and $m_{1/2} \simeq 1050$–1100 GeV (1200–1250 GeV) for $\tan\beta = 40$, respectively.

The strips within which the relic LSP density $\Omega_\chi h^2$ falls inside the range allowed by the available astrophysical and cosmological data for the total cold dark matter density $\Omega_{CDM} h^2$ are quite narrow, since $\Omega_{CDM} h^2$ is tightly constrained, at the % level, and the theoretical uncertainties in calculating $\Omega_\chi h^2$ are small within conventional big bang cosmology. However, we note that $\Omega_\chi h^2$ could be substantially smaller if the LSP is not the only important component of the cold dark matter. We therefore consider also the regions of the CMSSM parameter space with lower $\Omega_\chi h^2$ that have Δm smaller than along the coannihilation strips displayed in Fig. 1.

We return later to the other features exhibited in Fig. 1.

B. Review of $\tilde{\tau}$ decays

The starting point for the calculation of $\tilde{\tau}$ decays in the CMSSM is the $\tilde{\tau} - \chi - \tau$ Lagrangian, which was derived in detail in the Appendix of [12]. If $\Delta m > m_\tau$, the dominant decay mode is $\tilde{\tau}^- \to \tau^- \chi$, which gives a $\tilde{\tau}$ lifetime many orders of magnitude smaller than 1 nanosecond. If $\Delta m < m_\tau$, the three- and four-body decay modes,

---

[1]These choices of $\tan\beta$ and A_0 are also used in [12]. However, to avoid confusion when the reader compares the results of this paper with the previous one [12], where the SSARD code [26] was used, please note that here we use the opposite convention for the sign of A_0.
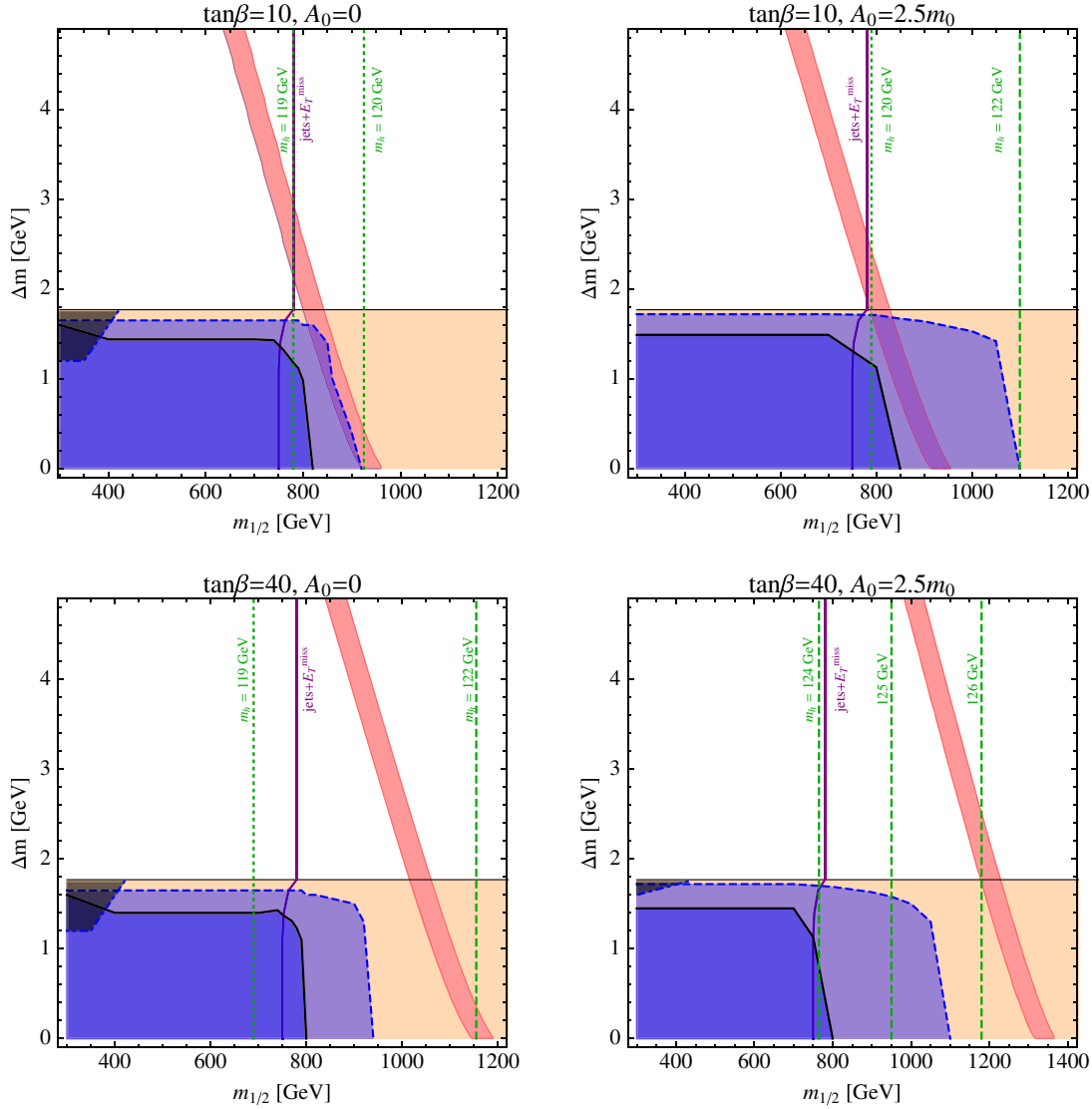
FIG. 1 (color online).　Overviews of the regions of the CMSSM parameter space with small mass difference $\Delta m \equiv m_{\tilde{\tau}} - m_{\chi}$ for $\tan\beta = 10$ (upper panels) and $\tan\beta = 40$ (lower panels), and for $A_0 = 0$ (left panels) and $2.5m_0$ (right panels). The bands with $\Delta m < m_{\tau}$ are shaded beige, and the coannihilation strips where $0.125 > \Omega_{\chi}h^2 > 0.115$ as calculated using SOFTSUSY 3.3.7 [23] coupled to MICROMEGAS 3.5.5 [24] are shaded pink. The lower limit on $m_{1/2}$ from the ATLAS E_T^{miss} search during Run 1 at the LHC [16] is represented in each panel by a maroon line, and contours of m_h calculated using FEYNHIGGS 2.10.0 [22] are shown as green (dashed or dotted) lines. Parameter regions excluded by searches for the direct and total production of metastable charged particles [15] are shaded darker and lighter blue, respectively, and regions excluded by searches for particles leaving disappearing tracks are shaded grey (see Sec. III for details).

$\tilde{\tau}^- \to a_1^-(1260)\nu_\tau\chi$, $\tilde{\tau}^- \to \rho^-(770)\nu_\tau\chi$, $\tilde{\tau}^- \to \pi^-\nu_\tau\chi$, $\tilde{\tau}^- \to \mu^-\bar{\nu}_\mu\nu_\tau\chi$ and $\tilde{\tau}^- \to e^-\bar{\nu}_e\nu_\tau\chi$, are the relevant ones, and their branching ratios varying with Δm, in particular. These channels close in sequence toward the tip of the coannihilation strip as $\Delta m \to 0$. Analytic expressions of the $\tilde{\tau}$ decay rates for these channels can be found in the Appendix of [12].

For 1.2 GeV $\lesssim \Delta m < m_{\tau}$, the $\tilde{\tau}$ lifetime is between order one and several hundred nanoseconds, so that the $\tilde{\tau}$ may decay in the outer part of the ATLAS and CMS detectors, and a disappearing track is the dominant $\tilde{\tau}$ signature.

Over most of this range of Δm, $\tilde{\tau}^- \to \rho^-(770)\nu_\tau\chi$ is the dominant decay mode with a branching ratio varying between $\sim$29% and $\sim$37%. The $\tilde{\tau}^- \to \pi^-\nu_\tau\chi$ branching ratio increases roughly linearly from $\sim$13% to $\sim$36% with the decrease of Δm, and it becomes the dominant mode at the lower end of Δm. The branching ratio of $\tilde{\tau}^- \to e^-\bar{\nu}_e\nu_\tau\chi$ is $\sim$18% to 20% over this Δm range, and $\tilde{\tau}^- \to \mu^-\bar{\nu}_\mu\nu_\tau\chi$ is $\sim$1% smaller than the former. The $\tilde{\tau}^- \to a_1^-(1260)\nu_\tau\chi$ branching ratio is about the same size as each of the four-body decay modes at $\Delta m \sim m_{\tau}$, decreasing to $\sim$5% at $\Delta m \sim 1.5$ GeV, and continually decreasing until its phase
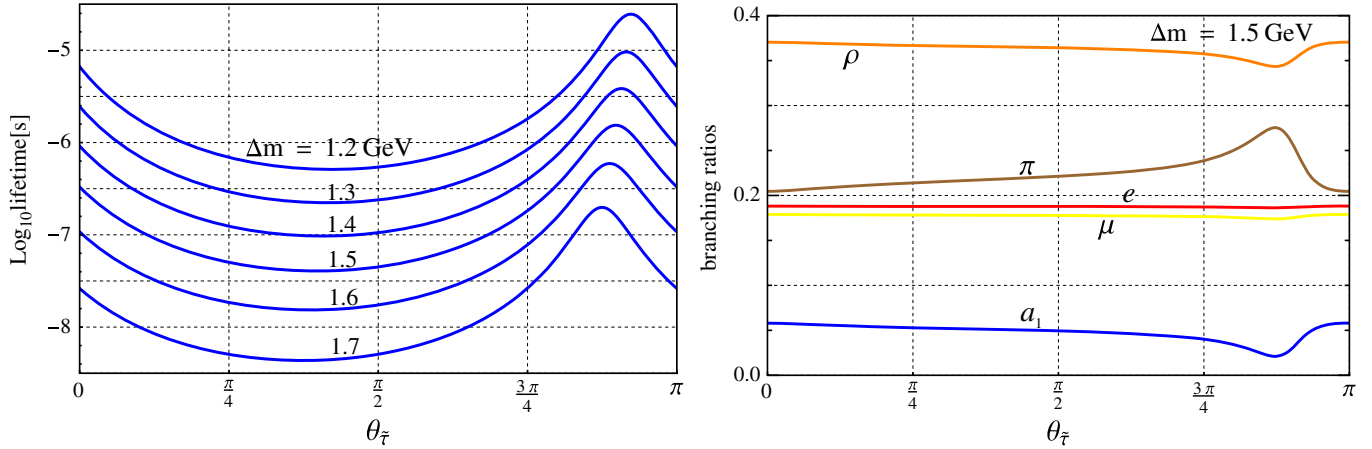
FIG. 2 (color online).   Left panel: the $\tilde{\tau}$ lifetime as a function of the $\tilde{\tau}_L - \tilde{\tau}_R$ mixing angle, $\theta_{\tilde{\tau}}$, for $\Delta m = 1.2, 1.3, \cdots, 1.7$ GeV. Right panel: the $\tilde{\tau}$ decay branching ratios as functions of $\theta_{\tilde{\tau}}$ for $\Delta m = 1.5$ GeV. The blue, orange, brown, yellow, and red lines are for the final states with $a_1(1260)$, $\rho(770)$, π, μ, and e, respectively, indicated by the labels adjacent to the corresponding curves. In both panels, a pure binolike χ with a mass of 300 GeV is assumed.

space vanishes at $\Delta m = m_{a_1}$. For $\Delta m \lesssim 1.2$ GeV, the $\tilde{\tau}$ is sufficiently long-lived so that it leaves the detectors before decaying, and the signature would be a massive metastable charged particle.

The $\tilde{\tau}$ lifetime and decay branching ratios were plotted in Fig. 7 and 8 in [12]. In those figures the χ was assumed to be pure binolike with a mass of 300 GeV, and the $\tilde{\tau}_L - \tilde{\tau}_R$ mixing angle, $\theta_{\tilde{\tau}}$, was taken to be $\pi/3$. These parameters were chosen in order to compare with the results of an earlier paper [27] where some differences in the $\tilde{\tau}$ decay calculations were found. We note that along $\tilde{\tau}$ coannihilation strip within the CMSSM, the χ is almost a bino, and the $\tilde{\tau}$ is almost right-handed. To see the effects of $\theta_{\tilde{\tau}}$ on the $\tilde{\tau}$ lifetime and decay branching ratios, we plot in the left panel of Fig. 2 the $\tilde{\tau}$ lifetime as a function of $\theta_{\tilde{\tau}}$ for the same 300 GeV pure binolike χ and for $\Delta m = 1.2, 1.3, \cdots, 1.7$ GeV, and in the right panel we show the branching ratios *vs.* $\theta_{\tilde{\tau}}$ curves for the same χ parameters and for $\Delta m = 1.5$ GeV. In these plots, $\theta_{\tilde{\tau}} = \pi/2$ corresponds to a pure right-handed $\tilde{\tau}$. We only show the plots for $\theta_{\tilde{\tau}} \in [0, \pi]$ because adding a π to $\theta_{\tilde{\tau}}$ is equivalent to change the overall sign of the $\tilde{\tau} - \chi - \tau$ Lagrangian, and it has no effect for the $\tilde{\tau}$ decay rates calculations performed in [12]. We can see that the $\tilde{\tau}$ lifetime strongly depends on $\theta_{\tilde{\tau}}$, but this dependence is not as strong as that of on Δm. On the other hand, the branching ratios only mildly depend on $\theta_{\tilde{\tau}}$, and this is also true for other choices of Δm which we do not show here. Finally, we note that for a given Δm, the $\tilde{\tau}$ lifetime is roughly proportional to m_χ (so that it is roughly proportional to $m_{1/2}$ in the CMSSM due to the relation $m_\chi \sim 0.42 m_{1/2}$), while the branching ratios are not sensitive to m_χ.

Figure 3 shows the $\tilde{\tau}$ lifetime contours as functions of $m_{1/2}$ and Δm, for the range $m_{1/2} \in (300, 1400)$ GeV and $\Delta m \in (1.2, 1.7)$ GeV. For all the four choices of the

CMSSM parameters used in Fig. 1, within this small Δm range the χ is almost a bino, and the $\tilde{\tau}$ is almost right-handed. Therefore, the $\tilde{\tau}$ lifetime essentially only depends on Δm and m_χ (or, equivalently, $m_{1/2}$), so that the contours are almost identical for all the four choices of the CMSSM parameters. The widths of the contours in Fig. 3 span the dependence of the $\tilde{\tau}$ lifetime on $\tan\beta$ and A_0. One can check that the $\tilde{\tau}$ lifetimes at $m_{1/2} \sim 720$ GeV are consistent with the values shown in the left panel of Fig. 2 for $\theta_{\tilde{\tau}} \sim \pi/2$.
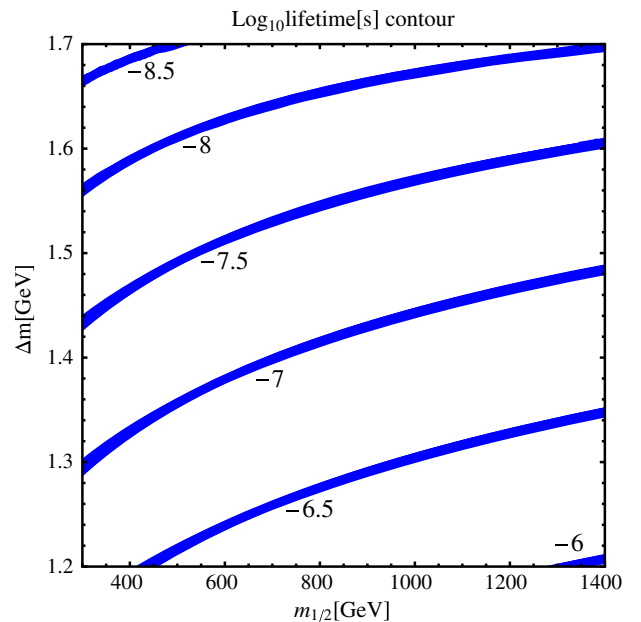

FIG. 3 (color online).   Some $\tilde{\tau}$ lifetime contours as functions of $m_{1/2}$ and Δm, for the four choices of the CMSSM parameters used in Fig. 1, namely, $\tan\beta = 10, 40$ and $A_0 = 0, 2.5 m_0$. The widths of the contours span ranges of the $\tilde{\tau}$ lifetime for the different choices of $\tan\beta$ and A_0.

III. THE IMPACTS OF THE LHC RUN 1 SEARCHES ON THE COANNIHILATION STRIP REGION

A. Searches for $E_T^{\rm miss}$ events

Both the ATLAS and CMS Collaborations have performed dedicated sets of experimental searches for generic new physics signatures with an abundance of missing transverse energy, $E_T^{\rm miss}$, as motivated in particular by supersymmetric models in which the stable lightest supersymmetric particle, commonly chosen to be the neutralino, is a massive dark matter particle. The signatures studied generally include jets, which could originate, e.g., from the pair production and subsequent cascade decays of squarks and gluinos. These searches have been carried out for a range of different final states, some including reconstructed leptons as well as jets tagged as originating from b-quarks, for a number of different ranges of the missing transverse energy and the total transverse energy. None of these searches found any significant evidence for new physics exhibiting these signatures in the LHC Run 1 data.

The ATLAS Collaboration has provided an interpretation of their data in the context of the CMSSM based on the 2012 dataset of 20/fb at a center of mass energy of 8 TeV [16]. The interpretation is presented in the $(m_0, m_{1/2})$ plane for a fixed value of $\tan\beta = 30$ and $A_0 = 2m_0$ (in our convention for the sign of A_0). Several different searches have been discussed in [16], but for the purposes of our study we concentrate on the 0-lepton search with 2–6 jets, as this provides the most stringent limit in the region of the stau coannihilation strip, and is also relatively insensitive to the values of $\tan\beta$ and A_0, as shown in a previous study [25]. As is shown by ATLAS, the CMSSM interpretation of this search provides a limit $m_{1/2} > 780$ GeV at the 95% C.L. near the stau coannihilation strip where $\Delta m > m_\tau$.[2]

We reproduce the ATLAS analysis in [16] using PYTHIA 8 with realistic smearing functions [28] to take into account detector effects, paying particular attention to the signal efficiencies of simulated points in the CMSSM parameter space close to the stau-coannihilation strip. We have considered the various signal regions defined for the ATLAS search, and studied how the different signal region efficiencies change as functions of the stau-neutralino mass splitting.

In the stau-coannihilation region, we find the strongest exclusions in the three-jet channel ($3j$) and four-jet channels ($4jt$), in agreement with the ATLAS analysis [16]. Our simulation results in a limit on $m_{1/2} > (780, 830)$ GeV in the signal regions $3j$ and $4jt$ (as defined in [16]) for the same choice of parameters and agrees well with the upper limits of $m_{1/2} > (780, 840)$ GeV reported in the

conference note [29] together with the analysis referred above. Combining this study with knowledge of the cross section, we extrapolate the ATLAS limit into the region where $\Delta m < m_\tau$.

This search requires tight cuts on missing transverse energy ($E_T^{\rm miss}$) and the effective mass ($m_{\rm eff}$) defined as the sum of the p_T of all jets plus the $E_T^{\rm miss}$. To investigate the variation in sensitivity of this search channel, we compare the distributions in these two variables for Δm above and below m_τ. As can be seen in the scatter plot in Fig. 4, there are events satisfying the ATLAS $4jt$ cuts even when $\Delta m = 0.5$ GeV and the stau is nearly stable (red points), albeit with a smaller efficiency than for $\Delta m = 1.9$ GeV (blue points). A similar effect is observed in the $3j$ signal region on which ATLAS exclusions in this region are based. We quantify in Sec. IV the sensitivity of this search for small Δm, in conjunction with the other searches discussed in Secs. III B and III C.

B. Searches for metastable charged particles

For stau lifetimes longer than a few nanoseconds, a significant fraction of staus lives long enough to escape the detector leaving a charged track signature. We can also use the 95% upper limits on long-lived charged particles at 8 TeV reported by CMS [15] to determine exclusions for small stau-neutralino mass differences Δm. The upper limits for direct production of stau pairs are between 4.3 fb for a stau mass of 126 GeV and 0.26 fb at 494 GeV, after which the limit plateaus. The limits for direct + indirect production (i.e., via cascade decays of other sparticles) are similar. For masses between 126 and 308 GeV, we interpolate using the discrete set of values given in [15], and beyond this we assume an upper limit of 0.3 fb, as suggested by the middle left panel of Fig. 8 of [15].

We calculate the fraction of events with at least one stau that is long-lived enough to escape the CMS detector, but exits within the central region $|\eta| < 2.1$ so that a track would be visible. Since the CMS upper limit constrains the total cross section, applying this limit to the restricted range of $|\eta|$ is slightly conservative. We find that a significant fraction of the staus with $\Delta m < 1.4$ GeV are stable on the scale of the CMS detector. We can rule out all $m_{1/2}$ values up to about 700 GeV, corresponding to $m_\chi = 291$ GeV, for $\Delta m < 1.4$ GeV by the direct production constraint. The excusion tapers off for $\Delta m > 1.4$ GeV, as can be seen in Fig. 1. The maximum $m_{1/2}$ ruled out at low Δm is between 800 and 850 GeV, which corresponds to a stau mass of 336–345 GeV. This agrees with the lower limit of 339 GeV for the mass of a stable stau established by the CMS direct search constraint.

When looking at both direct and indirect production, the search is sensitive to $\Delta m < 1.6$ GeV for $A_0 = 0$ and $\Delta m < 1.7$ GeV for $A_0 = 2.5 m_0$. The maximum $m_{1/2}$ exclusion is between 930 GeV (for $\tan\beta = 10$, $A_0 = 0$) and 1100 GeV for both values of $\tan\beta$ with $A_0 = 2.5 m_0$. This corresponds

---

[2]We note that the analogous CMS $E_T^{\rm miss}$ analysis could provide a similar sensitivity to the CMSSM parameters, but a CMSSM interpretation is not provided.
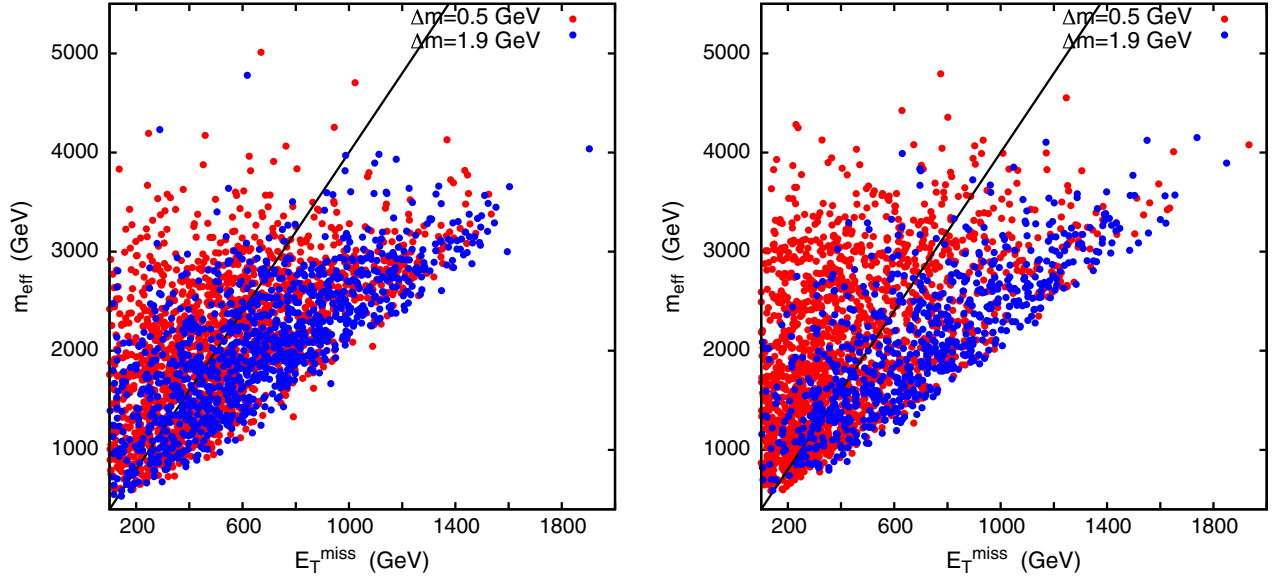
FIG. 4 (color online).   Scatter plot of E_T^{miss} and m_{eff} in the four-jet channel for CMSSM scenarios with metastable staus ($\Delta m = 0.5$ GeV, red points) and with rapid $\tilde{\tau} \to \tau + \chi$ decays ($\Delta m = 1.9$ GeV, blue points). The left plot is for $\tan\beta = 10$, $A_0 = 0$ and the right plot is for $\tan\beta = 40$, $A_0 = 2.5 m_0$, both with $m_{1/2} = 800$ GeV. The solid diagonal lines correspond to the ATLAS cut $E_T^{\mathrm{miss}} > 0.25 m_{\mathrm{eff}}$ [16].

to stau masses between 385 and 447 GeV and is conservative compared to the corresponding upper limit reported by CMS of 500 GeV.

C. Searches for disappearing tracks

The disappearing track search by the ATLAS Collaboration looks for well-defined tracks that do not proceed beyond the transition radiation tracker (TRT) region of the detector. This corresponds to a radial range of 563–1066 mm and a pseudorapidity range of $|\eta| < 2.0$. We simulate all event selection cuts in [17], namely (1) $E_T^{\mathrm{miss}} > 70$ GeV, (2) $p_T^{\mathrm{jet_1}} > 80$ GeV and (3) $\Delta\phi_{\mathrm{min}}^{\mathrm{jet}-E_T^{\mathrm{miss}}} > 1.0$. Several further cuts are applied to the stau track—(1) we require the track to be isolated by demanding that the sum of the p_T of all charged tracks within a cone of 0.4 around the stau track is less than 0.04 times the p_T of the track, (2) the candidate track has $p_T > 15$ GeV and is the highest p_T track in the event, and (3) the track has pseudorapidity in the range $0.1 < |\eta| < 1.9$. For the disappearing track criterion, we demand that the stau decays within the radial and pseudorapidity range of the TRT detector.

After applying all the cuts, we validate our simulation by reproducing to within 10% the efficiency for the benchmark anomaly mediated supersymmetry-breaking (AMSB) point reported in the analysis. As seen from Fig. 3, a value of Δm between 1.4 and 1.77 GeV results in stau lifetimes between 1 and 100 ns, which is the ideal range for disappearing-track signatures at the LHC.

The 95% cross-section upper limits reported by ATLAS for events with $p_T^{\mathrm{track}} > 75$, 100, 150 and 200 GeV are 1.76,

1.02, 0.62 and 0.44 fb, respectively, which we apply to the cross section for events passing all the cuts (1), (2) and (3) enumerated above. We find that restricting to direct-stau production does not yield any exclusions for $m_{1/2} > 300$ GeV. However, including both direct and indirect production, a small region below $m_{1/2} = 400$ GeV is ruled out for $\Delta m > 1.2$ GeV for $A_0 = 0$ and for $\Delta m > 1.6$ GeV for $A_0 = 2.5 m_0$. The jets $+ E_T^{\mathrm{miss}}$ search described above provides much stronger constraints for such values of Δm, excluding $m_{1/2} < 760$ GeV in this region.

IV. COMBINATION OF LHC CONSTRAINTS

We now discuss the interplay of the various LHC constraints displayed in Fig. 1. The solid maroon lines mark the boundary of the region still allowed following the ATLAS E_T^{miss} searches at 8 TeV. As discussed previously, the most relevant search is that for jets $+ E_T^{\mathrm{miss}}$, which provides a limit at $m_{1/2} = 780$ GeV in the region where $\Delta m > m_\tau$. This constraint is weakened when $\Delta m < m_\tau$, as discussed earlier.

The fraction of staus in the final state depends on the cascade decay branching ratios of the heavier sparticles, which depend in turn on the CMSSM parameters, as seen in Fig. 5. For $\tan\beta = 40$ and $A_0 = 2.5 m_0$, for example, both the second lightest neutralino, χ_2^0, and the lighter chargino, $\chi_1^\pm$, decay almost entirely into final states containing a stau, whereas for $\tan\beta = 10$ and $A_0 = 0$ they decay into staus in only about 20% and 64% of the cases, respectively. However, even when the stau lifetime is long enough that most staus escape the detector, sensitivity to E_T^{miss} is lost
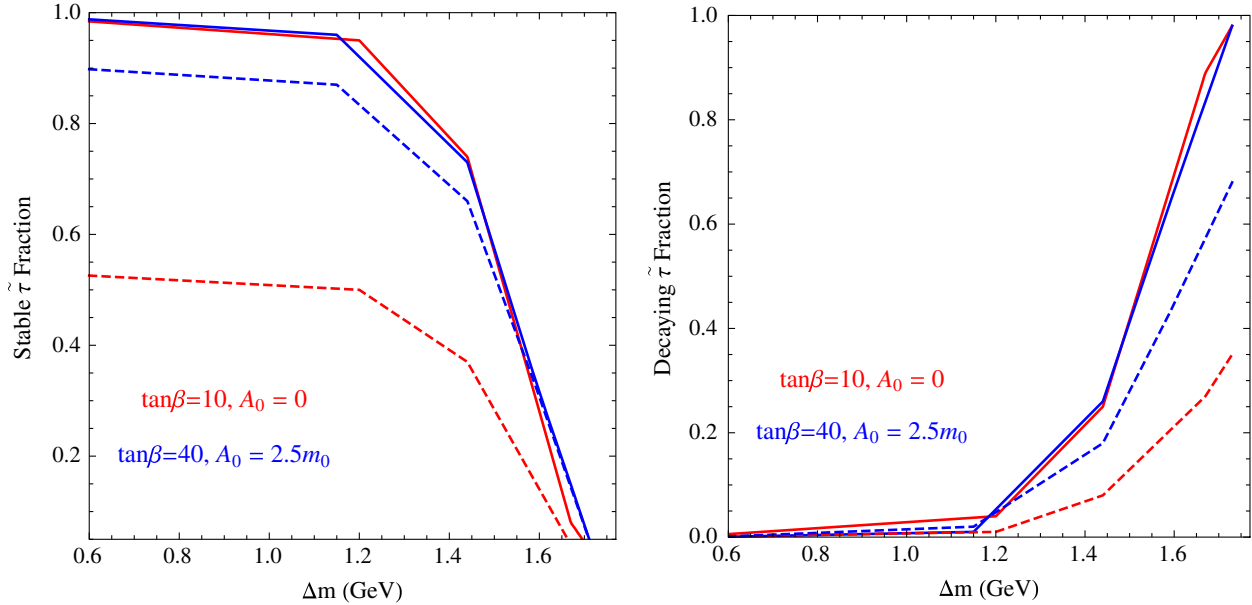
FIG. 5 (color online). The dependence of the fraction of 'stable' staus, i.e., those exiting CMS without decaying (left), and the fraction of staus decaying within the ATLAS detector (right) on the $\tilde{\tau} - \chi$ mass difference. The solid lines correspond to direct stau-pair production only whereas the dashed are for both direct and indirect stau production (i.e., all SUSY processes). The value of $m_{1/2}$ is fixed to 800 GeV.

only if the decay chains of *both* the produced sparticles result in staus. The dependence on Δm of the fraction of staus stable enough to exit the CMS detector is shown in the left panel of Fig. 5. As expected, we find that for small Δm, most staus are stable. The dashed lines (which correspond to the stau fraction from both direct and indirect production) asymptote to the total stau fraction in the final states as $\Delta m \to 0$. As Δm increases, the fraction of stable staus decreases until it becomes zero at the tau mass threshold. We find that when all production processes and decay chains are taken into account, the loss in efficiency for the E_T^{miss}-based search does not differ significantly for different values of $\tan \beta$ and A_0, and the limit $m_{1/2} > 780$ GeV given in [16] reduces to about 750 GeV.

We find that the most important constraint in the band where $\Delta m < m_\tau$ is that due to the search for metastable charged particles, shown by the shaded blue regions in Fig. 1. The darker shading is the constraint from direct stau pair production, and the lighter shading is that obtained by including indirect stau production via the cascade decays of heavier sparticles. The direct constraint yields a lower limit $m_{1/2} \gtrsim 700$ GeV for $\Delta m \lesssim 1.4$ GeV, which is only weakly sensitive to $\tan \beta$ but becomes stronger for $\Delta m \lesssim 1$ GeV when $A_0 = 2.5 m_0$. The indirect constraint yields a lower limit that is somewhat more sensitive to both $\tan \beta$ and A_0, yielding a lower limit $m_{1/2} \gtrsim 800$ to 1100 GeV.

As can be seen from the right panel of Fig. 5, the search for disappearing tracks becomes relevant for $m_\tau > \Delta m \gtrsim 1.2$ GeV. However, as already noted, it is weaker

than the other constraints, yielding $m_{1/2} \gtrsim 400$ GeV. This is mainly because, even with a significant fraction of staus decaying before exiting the detector, the signal efficiency for this search is of the order of 0.1–0.01% after implementing the cuts enumerated in Sec. III C.

In the case of $\tan \beta = 10$, for both $A_0 = 0$ and $2.5 m_0$ we see that the portions of the coannihilation strips with $\Delta m \gtrsim 3$ GeV are excluded by the ATLAS jets $+ E_T^{\text{miss}}$ search, whereas the portions with $3 \text{ GeV} \gtrsim \Delta m > m_\tau$ are allowed by this search. For $\tan \beta = 40$ and $A_0 = 0 (2.5 m_0)$ the portion of the strip where 6 GeV (9 GeV) $\gtrsim \Delta m > m_\tau$ is allowed by this search. When $\Delta m < m_\tau$, we see that none of the strips for $\tan \beta = 10, A_0 = 0$ or $\tan \beta = 40$ and $A_0 = 0$ or $2.5 m_0$ can be excluded, whereas for $\tan \beta = 10$ and $A_0 = 2.5 m_0$ the portion of the strip with $\Delta m \lesssim 1.7$ GeV is excluded by the search for massive charged particles.

In the ranges of $m_{1/2}$ exhibited in Fig. 1, FEYNHIGGS 2.10.0 generally yields values of m_h below the value measured at the LHC. Taking into account the uncertainties in the theoretical calculation of m_h, points yielding a nominal value ~ 122.5 GeV should probably not be regarded as excluded. Even taking this uncertainty into account, only the case $\tan \beta = 40, A_0 = 2.5 m_0$ is consistent with the LHC measurement of m_h.[3]

---

[3]We have checked that the value of m_h calculated using SOFTSUSY 3.3.7 is ~ 1.5 GeV smaller than the value given by FEYNHIGGS 2.10.0 for the parameter ranges presented in Fig. 1. This difference is within the latter code's uncertainties.

V. THE POTENTIAL REACHES OF FUTURE LHC SEARCHES

In order to extrapolate the potential reach of each of the three distinct categories of searches used in the analysis of this paper, we make a simple but, we believe, reasonable assumption, namely that the expected cross-section sensitivities of the respective searches will remain the same when going from a center-of-mass energy of 8 TeV to 13 or 14 TeV. Based on this assumption, we use PYTHIA 8 [18,19] to recalculate the cross sections in this higher center-of-mass regime and extrapolate the mass limit by requiring that, at the new mass limit, the cross section multiplied by the respective integrated luminosity is the same as for the Run 1 LHC data. The results of applying this hypothesis are shown in Fig. 6.

Figure 6 compares the prospective limits with the tip of the stau coannihilation strip for $\tan\beta = 40$ and $A_0 = 2.5m_0$, which was shown in Fig. 1 to be the most difficult to exclude. We do not display the projected sensitivity of the 'disappearing track' search, which we do not expect to be competitive because of its low efficiency, as discussed earlier. We see that the projected sensitivity of the jets $+ E_T^{\text{miss}}$ search is ~1700 GeV for $\Delta m > m_\tau$, decreasing to ~1650 GeV for $\Delta m < 1.6$ GeV,

which is sufficient to explore all the coannihilation strip. The most sensitive search channel when $\Delta m \lesssim 1.6$ GeV is expected to be that for massive charged particles, which would also be strong enough to explore independently this portion of the coannihilation strip: its sensitivity should reach ~1850 GeV for very small Δm. The combination of these searches would clearly explore thoroughly the CMSSM coannihilation strip in this and, *a fortiori*, the other cases we study. Indeed, we estimate the tip of the strip at $m_{1/2} \sim 1400$ GeV can be explored with 75/fb data at 14 TeV. Points within the stau coannihilation strip could be detected in two ways, via their E_T^{miss} and massive stable particle signatures. Conversely, the absence of signals in both these channels would exclude robustly the stau coannihilation strip.

VI. CONCLUSIONS

We have analyzed in this paper the impacts on the CMSSM parameter space in the neighbourhood of the tip of the stau coannihilation strip of various LHC searches, including the ATLAS jets $+ E_T^{\text{miss}}$ search, the CMS search for massive charged particles, and the ATLAS search for disappearing tracks, which are sensitive in different regions of Δm and $m_{1/2}$. We have found that the jets $+ E_T^{\text{miss}}$ search has important sensitivity when $\Delta m < m_\tau$, though the strongest constraint for small Δm is generally that provided by the search for massive charged particles. The search for disappearing tracks has impact only for $\Delta m \gtrsim 1.6$ GeV, where it is considerably less sensitive than the jets $+ E_T^{\text{miss}}$ search.

We have studied four CMSSM cases, with the following conclusions. For $\tan\beta = 10$ and $A_0 = 0$, the portion of the coannihilation strip with $\Delta m \gtrsim 3$ GeV is excluded by the jets $+ E_T^{\text{miss}}$ search, but the portion with $\Delta m \lesssim 3$ GeV cannot yet be excluded. For $\tan\beta = 10$ and $A_0 = 2.5m_0$, the portion of the coannihilation strip with $\Delta m \gtrsim 3$ GeV is again excluded by the jets $+ E_T^{\text{miss}}$ search, and the portion with $\Delta m \lesssim 1.7$ GeV is excluded by the search for massive charged particles, but there is no exclusion for the portion with 1.7 GeV $\lesssim \Delta m \lesssim 3$ GeV. For $\tan\beta = 40$ and $A_0 = 0$, only the portion of the coannihilation strip with $\Delta m \gtrsim 6$ GeV is excluded, again by the jets $+ E_T^{\text{miss}}$ search, and there is no exclusion for $\Delta m < m_\tau$. Finally, for $\tan\beta = 40$ and $A_0 = 2.5m_0$, only the portion of the coannihilation strip with $\Delta m \gtrsim 9$ GeV is excluded, again by the jets $+ E_T^{\text{miss}}$ search.

We have also projected the likely sensitivities of the LHC searches in Run 2 of the LHC at energies approaching 14 TeV and with up to 300/fb of integrated luminosity. We find that a combination of the jets $+ E_T^{\text{miss}}$ and massive charged particle searches should be able to explore robustly the entire CMSSM coannihilation strip for all the cases we have studied. The end of the CMSSM coannihilation strip is indeed nigh, one way or another.
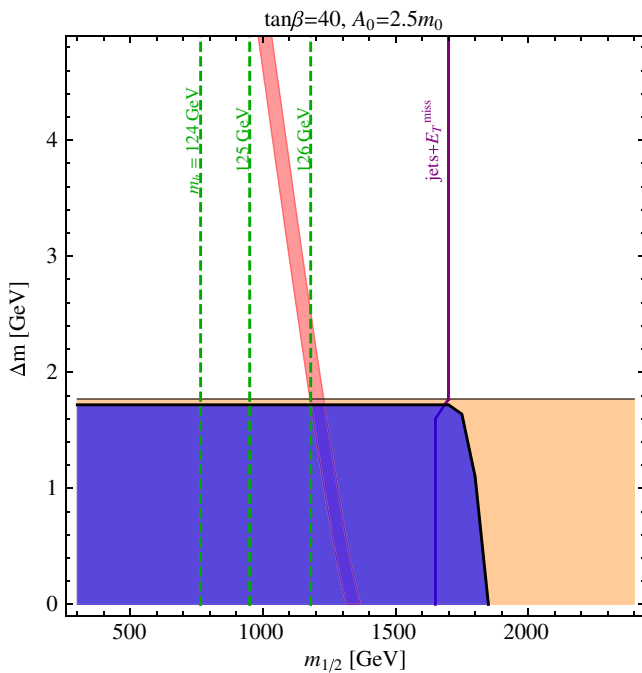

FIG. 6 (color online). Projected limits from the 14 TeV LHC Run 2 with 300/fb integrated luminosity. The sensitivity of the jets $+ E_T^{\text{miss}}$ search is sufficient to explore the rest of the coannihilation strip, and the search for metastable charged tracks from direct stau-pair production is also strong enough to explore independently the portion of the coannihilation strip where $\Delta m \lesssim 1.6$ GeV.

---

[1] ATLAS Collaboration, https://twiki.cern.ch/twiki/bin/view/AtlasPublic/SupersymmetryPublicResults.

[2] CMS Collaboration, https://twiki.cern.ch/twiki/bin/view/CMSPublic/PhysicsResultsSUS.

[3] H. Goldberg, Phys. Rev. Lett. **50**, 1419 (1983); J. Ellis, J. Hagelin, D. Nanopoulos, K. Olive, and M. Srednicki, Nucl. Phys. **B238**, 453 (1984).

[4] E. Komatsu et al. (WMAP Collaboration), Astrophys. J. Suppl. Ser. **192**, 18 (2011).

[5] P. A. R. Ade et al. (Planck Collaboration), arXiv:1303.5076.

[6] M. Drees and M. M. Nojiri, Phys. Rev. D **47**, 376 (1993); H. Baer and M. Brhlik, Phys. Rev. D **53**, 597 (1996); Phys. Rev. D **57**, 567 (1998); H. Baer, M. Brhlik, M. A. Diaz, J. Ferrandis, P. Mercadante, P. Quintana, and X. Tata, Phys. Rev. D **63**, 015007 (2000).

[7] G. L. Kane, C. F. Kolda, L. Roszkowski, and J. D. Wells, Phys. Rev. D **49**, 6173 (1994); J. R. Ellis, T. Falk, K. A. Olive, and M. Schmitt, Phys. Lett. B **388**, 97 (1996); Phys. Lett. B **413**, 355 (1997); J. R. Ellis, T. Falk, G. Ganis, K. A. Olive, and M. Schmitt, Phys. Rev. D **58**, 095002 (1998); V. D. Barger and C. Kao, Phys. Rev. D **57**, 3131 (1998); J. R. Ellis, T. Falk, G. Ganis, and K. A. Olive, Phys. Rev. D **62**, 075010 (2000).

[8] J. Ellis, T. Falk, and K. A. Olive, Phys. Lett. B **444**, 367 (1998); J. Ellis, T. Falk, K. A. Olive, and M. Srednicki, Astropart. Phys. **13**, 181 (2000); **15**, 413(E) (2001).

[9] C. Boehm, A. Djouadi, and M. Drees, Phys. Rev. D **62**, 035012 (2000); J. R. Ellis, K. A. Olive, and Y. Santoso, Astropart. Phys. **18**, 395 (2003); J. Ellis, K. A. Olive, and J. Zheng, arXiv:1404.5571.

[10] A. B. Lahanas, D. V. Nanopoulos, and V. C. Spanos, Mod. Phys. Lett. A **16**, 1229 (2001); A. B. Lahanas and V. C. Spanos, Eur. Phys. J. C **23**, 185 (2002); J. R. Ellis, T. Falk, G. Ganis, K. A. Olive, and M. Srednicki, Phys. Lett. B **510**, 236 (2001).

[11] J. L. Feng, K. T. Matchev, and T. Moroi, Phys. Rev. Lett. **84**, 2322 (2000); Phys. Rev. D **61**, 075005 (2000); J. L. Feng, K. T. Matchev, and F. Wilczek, Phys. Lett. B **482**, 388 (2000).

[12] M. Citron, J. Ellis, F. Luo, J. Marrouche, K. A. Olive, and K. J. de Vries, Phys. Rev. D **87**, 036012 (2013).

[13] T. Cohen and J. G. Wacker, J. High Energy Phys. 09 (2013) 061.

[14] Y. Konishi, S. Ohta, J. Sato, T. Shimomura, K. Sugai, and M. Yamanaka, Phys. Rev. D **89**, 075006 (2014).

[15] S. Chatrchyan et al. (CMS Collaboration), J. High Energy Phys. 07 (2013) 122.

[16] G. Aad et al. (ATLAS Collaboration), arXiv:1405.7875.

[17] G. Aad et al. (ATLAS Collaboration), Phys. Rev. D **88**, 112006 (2013).

[18] T. Sjostrand, S. Mrenna, and P. Z. Skands, Comput. Phys. Commun. **178**, 852 (2008).

[19] N. Desai and P. Z. Skands, Eur. Phys. J. C **72**, 2238 (2012).

[20] G. Aad et al. (ATLAS Collaboration), Phys. Lett. B **716**, 1 (2012).

[21] S. Chatrchyan et al. (CMS Collaboration), Phys. Lett. B **716**, 30 (2012).

[22] T. Hahn, S. Heinemeyer, W. Hollik, H. Rzehak, and G. Weiglein, Phys. Rev. Lett. **112**, 141801 (2014).

[23] B. C. Allanach, Comput. Phys. Commun. **143**, 305 (2002).

[24] G. Belanger, F. Boudjema, A. Pukhov, and A. Semenov, Comput. Phys. Commun. **185**, 960 (2014); **174**, 577 (2006); **149**, 103 (2002).

[25] O. Buchmueller, R. Cavanaugh, M. Citron, A. De Roeck, M. J. Dolan, J. R. Ellis, H. Flacher, S. Heinemeyer et al., Eur. Phys. J. C **72**, 2243 (2012); see also O. Buchmueller, R. Cavanaugh, A. De Roeck, M. J. Dolan, J. R. Ellis, H. Flacher, S. Heinemeyer, G. Isidori et al., Eur. Phys. J. C **74**, 2922 (2014).

[26] Information about this code is available from K. A. Olive; it contains important contributions from T. Falk, A. Ferstl, G. Ganis, F. Luo, A. Mustafayev, J. McDonald, K. A. Olive, P. Sandick, Y. Santoso, and M. Srednicki.

[27] T. Jittoh, J. Sato, T. Shimomura, and M. Yamanaka, Phys. Rev. D **73**, 055009 (2006).

[28] S. Chatrchyan et al. (CMS Collaboration), Report No. CMS-DP-2013-003; Report No. CMS-DP-2013-033; JINST **8**, P09009 (2013); **7**, P10002 (2012).

[29] The ATLAS Collaboration, Report No. ATLAS-CONF-2013-047, http://atlas.web.cern.ch/Atlas/GROUPS/PHYSICS/CONFNOTES/ATLAS-CONF-2013-047/.